Polyoxometalates

Assembly of Molecular "Layered" Heteropolyoxometalate Architectures**

Jing Gao, Jun Yan, Sebastian Beeg, De-Liang Long,* and Leroy Cronin*

Heteropolyoxometalates (HPOMs) and lacunary HPOMs are the most explored subset of polyoxometalates (POMs) which contain heteroanion templates.[1–4] Lacunary HPOMs are particularly important since they can be used as building blocks to construct much larger structures of nanoscale dimensions. Most of the previous reports on lacunary HPOMs are based upon "conventional" heteroanion templates (e.g. SiO_4^{4-}, PO_4^{3-}, SO_4^{2-}, AsO_4^{3-}) which are redox-inactive. However HPOMs with anion templates that have the possibility of themselves being redox active have been far less explored.[3] During the past few years we have been targeting HPOMs with redox active heteroanions (e.g. SO_3^{2-}, TeO_3^{2-}, SeO_3^{2-}) in an effort to engineer clusters with intrinsically more diverse structures and redox active properties.[5–8] However a general building block strategy based upon lacunary HPOMs with non-conventional anions has not been developed.

Herein we report a strategy of constructing a "layered" molecular assembly in constructing a new family of Te^{IV}-containing HPOM building blocks which consist of a $\{W_3\}$ top unit and one, two, and three layers of $\{TeW_6\}$ base units in $[TeW_9O_{33}]^{8-}$, $[Te_2W_{15}O_{54}]^{10-}$, and $[Te_3W_{21}O_{75}]^{12-}$, respectively, Further, the principal axis of the TeO_3^{2-}, on which the lone-pair of electrons is located, are all orientated in the same direction towards the open end of the lacunary HPOM cluster (Figure 1).

In this work, the self-assembly of the three lacunary HPOM building blocks mentioned above yielded three polyanion types: $[Pd_3(TeW_9O_{33})_2]^{10-}$ (**1a**) in the form of $Na_2K_8[Pd_3(TeW_9O_{33})_2]\cdot 51H_2O$ (**1**); $[(WO_2)_4(Te_2W_{15}O_{54})_4]^{32-}$ in the two isomeric forms **2a** and **2a′** which can be formulated as $(C_2H_8N)_{19}Na_{13}[(WO_2)_4(Te_2W_{15}O_{54})_4]\cdot 57H_2O$ (**2**) and $(C_2H_8N)_{19}Cs_2Na_{11}[(WO_2)_4(Te_2W_{15}O_{54})_4]\cdot 77H_2O$ (**2′**); $[Te_3W_{21}O_{75}]^{12-}$ (**3a**) in the form of $(C_2H_8N)_8Na_4[Te_3W_{21}O_{75}]\cdot 25H_2O$ (**3**). In addition to the structural studies, these clusters have also been explored using electrospray ionization mass spectrometry and cyclic voltammetry confirming stability and revealing interesting electronic properties.

[*] J. Gao, Dr. J. Yan, S. Beeg, Dr. D. L. Long, Prof. L. Cronin
WestCHEM, School of Chemistry, The University of Glasgow
University Avenue, Glasgow G12 8QQ (UK)
E-mail: deliang.long@glasgow.ac.uk
           lee.cronin@glasgow.ac.uk
Homepage: http://www.croninlab.com

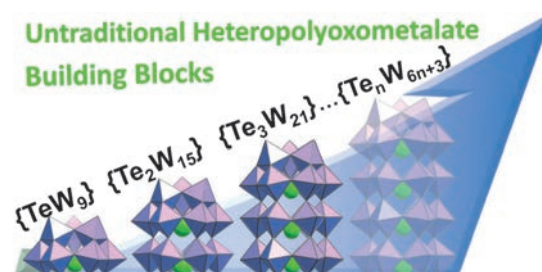Supporting information for this article is available on the WWW under http://dx.doi.org/10.1002/anie.201108428.

Figure 1. New members of the one-, two-, and three-layered Te^{IV}-containing HPOM "pagoda" reported here; note the faded four-layered structure is hypothetical. Purple octahedron: $\{WO_6\}$; green spheres: Te.

Compound **1** was synthesized by a simple one-pot reaction of Na_2WO_4, TeO_2, $Pd(NO_3)_2\cdot H_2O$ in a weakly acidic aqueous solution at 95°C. The X-ray crystal structure analysis of **1a** reveals three square-coordinated Pd^{II} ions are sandwiched between two B-β-$\{Te_9O_{33}\}$ subunits (Figure 2). The average Pd^{II}—O bond lengths are 1.999(19) Å which is in agreement with the literature.[9] Compound **1** together with those previously reported examples[10–12] confirmed the one-layered building block $[TeW_9O_{33}]^{8-}$ could be easily obtained in the presence of transition metal ions. To find new "pure" Te-containing HPOM building blocks, we then conducted similar one-pot reaction of only $Na_2WO_4\cdot 2H_2O$, Na_2TeO_3, and H_2O with a pH value of 4.6 in the presence of dimethylammonium (DMA) at room temperature, from which the high nuclearity $\{Te_8W_{64}O_{224}\}$ compound **2** was isolated. X-ray crystal structure analysis of **2** reveals a topologically D_{2d}-symmetric $[(WO_2)_4(Te_2W_{15}O_{54})_4]^{32-}$ cluster anion **2a** (Figure 3 left). From Figure 3 (left) it can be seen that the cluster anion **2a**,

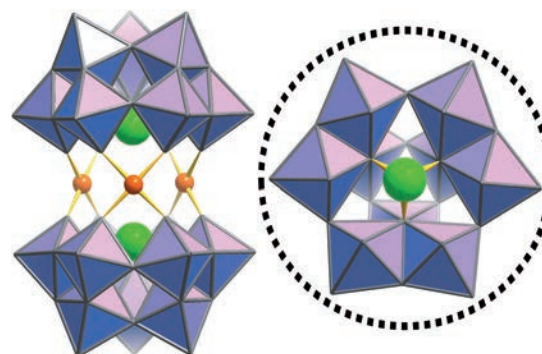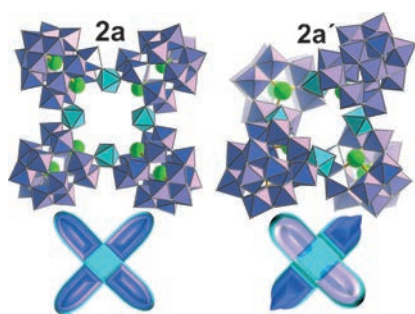*Figure 2.* Structure representation of the anion $[Pd_3(TeW_9O_{33})_2]^{10-}$ (**1a**). Left: front-view; right: $\{TeW_9O_{33}\}$ subunit; light purple octahedron: $\{WO_6\}$; green spheres: Te; orange spheres: Pd.

© 2012 Wiley-VCH Verlag GmbH & Co. KGaA, Weinheim

Figure 3. Structural representation of the anions {Te$_8$W$_{64}$O$_{224}$}$^{32-}$ = [(WO$_2$)$_4$(Te$_2$W$_{15}$O$_{54}$)$_4$]$^{32-}$ found as isomeric **2a** (left) and **2a′** (right). A schematic representation of the {TeW$_{15}$} subunits is below and shows the structural differences between the isomers. Light purple octahedron: {WO$_6$}; cyan octahedron: {WO$_6$} linker; green spheres: Te.

[Te$_8$W$_{64}$O$_{224}$]$^{32-}$, is tetrameric and consists of four {Te$_2$W$_{15}$O$_{54}$} subunits linked by four {WO$_6$} ({W$_1$}) groups, giving the anion a cyclic structure. Each {W$_1$} linker joins two {Te$_2$W$_{15}$O$_{54}$} subunits by sharing two *cis*-oxygen atoms while each {Te$_2$W$_{15}$O$_{54}$} subunit consists of a {W$_3$} top and two layers of {TeW$_6$O$_{21}$} pieces that are composed of a {W$_6$} planar ring templated by a pyramidal {TeO$_3$} group. The two {TeW$_6$O$_{21}$} layers in each {Te$_2$W$_{15}$O$_{54}$} subunit of compound **2** are connected together by corner-sharing oxygen ligands. It is very interesting to note that the {TeO$_3$} template in the first layer has the same orientation to that in the second layer and the oxo ligands in both templates are eclipsed, which distinguishes these {Te$_2$W$_{15}$O$_{54}$} subunits from all other traditional lacunary HPOM building blocks, for example, {P$_2$W$_{15}$} etc. derived from the Dawson parents. Further, since it is well known that nature of the charge balancing cations can have a profound effect on the self-assembly of POMs-based architectures, we explored the use of larger Cs$^+$ cations in the assembly of compound **2**. To our surprise, another compound **2′** with anion **2a′** which is a topological isomer to **2a** was isolated (Figure 3, right). For both **2a** and **2a′**, it is possible to define a plane containing the four {W$_1$} linkers, then it can be seen that the four hanging {W$_2$O$_9$} moieties in the second layer of each {Te$_2$W$_{15}$O$_{54}$} subunit in **2a** are distributed alternatively above and below the plane; however, the distribution has changed in **2a′** with all four hanging {W$_2$O$_9$} units lying at the same side of the plane, giving **2a′** approximately C_{4v} symmetric (although the cluster is geometrically C_{2v} symmetric; see Supporting Information, Figure S1). Also it should be noted that in both **2a** and **2a′**, each of the four {W$_1$} linkers have two terminal W=O bonds whose lengths vary in the same range from about 1.70(2) Å to 1.81(2) Å. Viewed from the front, it can be seen that **2a** is flatter than **2a′** since the maximum dimensions are ca. 2.9 nm long and 1.1 nm thick whereas these are 2.7 and 1.9 nm for **2a′** (see Figure S1).

Given the different cations used to assemble compounds **2** and **2′**, it is interesting to examine the cavities in the middle of **2a** and **2a′**. The former is occupied by a number of Na$^+$ ions and solvent water molecules while the latter is filled by disordered Cs$^+$ and Na$^+$ cations (Figure S2). Therefore it can be suggested that the planar middle cavity of **2a** is deformed

to reduce the steric hindrance which results in its structural rearrangement, giving transformation from planar **2a** to a saddle-shaped **2a′** (Figure 3). Building on the cation-controlled structures of **2** and **2′**, we also attempted to utilize smaller Li$^+$ cations in this reaction system which resulted in the formation of compound **3** containing the anion [Te$_3$W$_{21}$O$_{75}$]$^{12-}$ (**3a**; Figure 4). However, it should be pointed
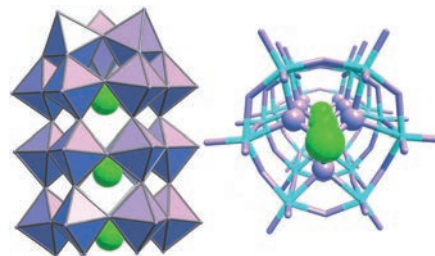
Figure 4. Side view (left) and bottom view (right) of [Te$_3$W$_{21}$O$_{75}$]$^{12-}$. Light purple octahedron: {WO$_6$}, green spheres: Te; light purple spheres: O.

out during our experimental exploration we found that Li$^+$ is not essential to form compound **3** and we were able to devise a synthetic route that did not require Li$^+$. Compared with the two-layered {Te$_2$W$_{15}$O$_{54}$} subunit contained in clusters **2a** and **2a′**, anion **3a** has a three-layered structure with one more layer {TeW$_6$O$_{21}$} added to {Te$_2$W$_{15}$O$_{54}$} (Figure 4). The {TeO$_3$} templates in each layer of **3a** oriented toward the same direction and all oxo ligands are eclipsed, the same as that in anion **2a** and **2a′**.

ESI-MS was utilized to explore the solution behavior of these compounds. The mass spectra of compound **1** in a mixture of deionized water and acetonitrile (5%: 95%) shows that the whole cluster {Pd$_3$(TeW$_9$O$_{33}$)$_2$} is present and all the main peaks can be assigned to its different charge/cation states (Figure S3 and Table S1). Further, the mass spectra of compounds **2** and **2′** are very similar: for each peak with the same charge, the *m/z* value of compound **2** is 58–70 mass units bigger than that of **2′** (Figure 5). Considering that both clusters **2** and **2′** have the same gross structure, the key difference lies with different species and numbers of cations, and crystalized water molecules. Both **2** and **2′** are observed as
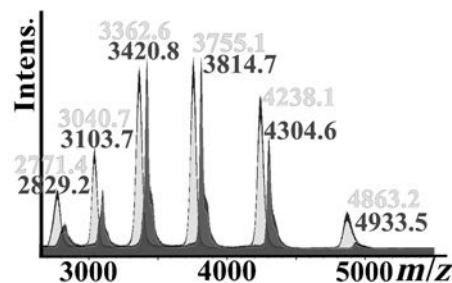

Figure 5. Negative-ion mode ESI of compound **2** (dark gray) and **2′** (light gray) in mixed H$_2$O/MeCN solvent (5%:95%). All the peaks shown in each spectrum relate to different states of the same basic parent cluster [Te$_8$W$_{64}$O$_{224}$]$^{32-}$, which are observed as either a monomer or a dimer in the gas phase.

an assembly of related clusters with differing numbers of cations and water molecules existing either as a $\{Te_8W_{64}O_{224}\}$ monomer or as a $\{Te_8W_{64}O_{224}\}_2$ dimer; for example, the monomer of **2a** can be assigned as $[H_{18+x}(C_2H_8N)_{4+y}Na_{4+z}(H_2O)_{17+n}(Te_8W_{64}O_{224})]^{(6-x-y-z)-}$ and the dimer as $[H_{33+x}(C_2H_8N)_{12+y}Na_{7+z}(H_2O)_{54+n}(Te_8W_{64}O_{224})_2]^{(12-x-y-z)-}$. Similarly, the monomer of **2a'** can be assigned as $[H_{23+x}(C_2H_8N)_{0+y}Na_{0+z}(CsNa_2)(H_2O)_{3+n}(Te_8W_{64}O_{224})_2]^{(6-x-y-z)-}$ and the dimer as $[H_{37+x}(C_2H_8N)_{3+y}Na_{6+z}(Cs_2Na_4)(H_2O)_{19+n}(Te_8W_{64}O_{224})_2]^{(12-x-y-z)}$ (see Tables S2 and S3).

It should be noted from the assignment of the mass spectrum of anion **2a'** that the number of the inorganic cations (one Cs^+ and two Na^+) occupying the middle cavity of **2a'** are double in all the dimer peaks compared to that in all the monomer peaks (Table S3), indicating that these inorganic cations are mainly responsible for the structural difference between polyanion **2a** and **2a'**. The assignments of polyanion **2a** and **2a'** were made possible due to their high charge, with assignments made via charge deconvolution. The ESI study of compound **3** in H₂O/MeCN solvent (5%:95%) shows that the expected $\{Te_3W_{21}O_{75}\}$ cluster anion is present and all the main peaks can be assigned to different charge/ cation states associated with the molecular species. The negative mode mass spectrum of compound **3** shows that there are four main peaks. Also all the peaks can be assigned as a three-layered dimer $\{Te_3W_{21}O_{75}\}_2$ (Table S4). This is a good indication that compound **3** can retain its structural integrity in solution, and shows the possibility that it might be an excellent precursor for functionalization.

It is well known that many HPOMs are highly redox-active,[2,3] thus cyclic voltammetry experiments were performed to examine the redox properties of compounds **2**, **2'**, and **3** in 0.1 M NaH₂PO₄/Na₂HPO₄ buffer solution, and these compounds display a range of different behaviors (Figures 6, S5 and S6). Between +0.257 to −0.700 V (vs. Ag/AgCl) all the compounds show waves associated with the reduction of tungstate centres. For compound **1**, only one quasi-reversible
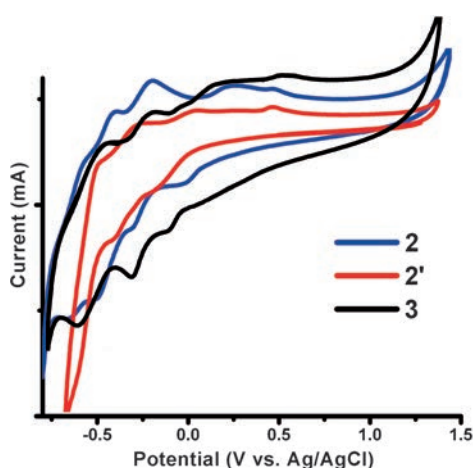
couple is observed with $E_{1/2}$ value located at −0.178 V because of the redox process of Pd^{II} ions (Figure S5). The oxidation peak at +0.810 V and the reduction peak at +0.200 V are related, which can be assigned to the redox process between Pd^{II} and Pd^{IV} couple.[13] Surprisingly, all the other spectra of the multi-layered clusters contain an oxidation peak at +0.500 V which can be assigned as the oxidation of Te^{IV}, and it does not shift by varying scan rates. However, the redox processes of tungstate showed many differences between compound **2** and **3** (Figures S7 and S11). Although in both cases, four quasi-reversible couples can be observed, the first wave is significantly positively shifted in compound **2** ($E_{1/2} = +0.137$ V in **2** vs. +0.104 V in **3**), while the other three peaks shifted towards the opposite direction (Figure 6). Furthermore, the topological isomers **2** and **2'** showed different redox behaviors with only two quasi-reversible waves appeared under the similar condition for compound **2'**, in which the first wave negatively moved around 220 mV ($E_{1/2} = -0.085$ V).

In summary, we have discovered a new family of "layered" tungstatotellurite compounds showing unique layered structures built from a series of untraditional Te^{IV}-containing POM building blocks, i.e., $[TeW_9O_{33}]^{8-}$, $[Te_2W_{15}O_{54}]^{10-}$, and $[Te_3W_{21}O_{75}]^{12-}$. The possibility to access "layered" clusters opens the door to more extended systems (e.g. for layers beyond 3 as depicted in Figure 1) and also the linking of the units allows the generation of nanostructured clusters whose gross conformation is cation controlled as demonstrated by compounds **2** and **2'** $\{Te_8W_{64}O_{224}\}$. In future work we will investigate the dynamic cation-mediated conformational switching of the nanoscale $\{Te_8W_{64}O_{224}\}$ cluster, as well as exploring the development of photo- and electrochemical properties of these and related clusters that exploit the incorporation of the Te heteroatom.

Experimental Section

Synthesis of 1: Na₂WO₄·2H₂O (1.00 g, 3.03 mmol) was dissolved in boiling water (40 mL), and a solution of TeO₂ (0.10 g, 0.63 mmol) in 2.5 M KOH solution (2 mL) was added dropwise to the tungstate solution. The pH of this mixture was adjusted to 7.0 by addition of 70% nitric acid, and the mixture was heated at 95°C for 25 min. Pd(NO₃)₂·H₂O (0.08 g, 0.43 mmol) was added to the solution, during which the pH was kept around 5.4 by using 2.5 M KOH. The solution was kept at 95°C under stirring for more 30 min, cooled, filtered and left to evaporate slowly. Dark red-brown block crystals of **1** appeared after two weeks. Yield: 0.17 g (16% based on W). IR (KBr disk): $\tilde{\nu} =$ 3449, 1623, 954, 887, 793, 743 cm⁻¹. Elemental analysis calcd for H₁₀₂K₈Na₂O₁₁₇Pd₃Te₂W₁₈ (%): K 5.03, Pd 5.13, W 53.2; found: K 5.12, Pd 5.17, W 53.0.

Synthesis of 2: Na₂WO₄·2H₂O (1.70 g, 5.15 mmol), Na₂TeO₃ (0.13 g, 0.58 mmol) and dimethylamine hydrochloride (0.7 g, 8.58 mmol) were dissolved in water (30 mL). The pH was first adjusted to 6.0 by addition of 50% acetic acid and then further to 4.6 by 37% HCl. Then the solution was filtered and left to evaporate slowly. Colorless block crystals of **2** appeared after three weeks. Yield: 0.26 g (17% based on W). IR (KBr disk): $\tilde{\nu} = 3408$, 3147, 2784, 2358, 1623, 1464, 1019, 966, 788, 713 cm⁻¹. Elemental analysis calcd for C₃₈H₂₆₆N₁₉Na₁₃O₂₈₁Te₈W₆₄ (%): C 2.46, H 1.44, N 1.43, Na 1.61, W 63.35; found: C 2.83, H 1.21, N 1.47, Na 1.68, W 63.3.

Synthesis of 2': The procedure is exactly the same as that for preparing **2** but before filtration for crystallization, CsCl (0.22 g, 1.31 mmol) was added in and then the solution was filtered and left to

Figure 6. Cyclic voltammograms of compounds **1**, **2**, **2'**, and **3** in 0.1 M NaH₂PO₄/Na₂HPO₄ buffer solution. The scan rate was 100 mVs⁻¹, the working electrode was glassy carbon (3 mm), and the reference electrode was Ag/AgCl.

evaporate slowly. Colorless block crystals of **2′** appeared within one week. Yield: 0.32 g (21 %). IR (KBr disk): $\tilde{\nu}=3423, 3147, 2785, 2358, 1631, 1464, 1019, 962, 789, 714$ cm^{-1}. Elemental analysis, calcd for $C_{38}H_{306}N_{19}Cs_2Na_{11}O_{301}Te_8W_{64}$ (%): C 2.38, H 1.61, N 1.39, Na 1.32, Cs 1.39, W 61.43; found: C 2.79, H 1.02, N 1.43, Na 1.31, Cs 2.45, W 61.4.

Synthesis of **3**: The procedure is exactly the same as that for preparing **2** but before filtration for crystallization, the solution was heated at around 85 °C for 30 min, cooled down to room temperature, filtered and left to evaporate slowly. Colorless block crystals of **3** appeared within two weeks. Yield: 0.34 g (22 % based on W). IR (KBr disk): $\tilde{\nu}=3419, 3155, 2441, 2784, 1627, 1464, 1019, 939, 797, 741$ cm^{-1}. Elemental analysis, calcd for $C_{16}H_{114}N_8Na_4O_{100}Te_3W_{21}$ (%): C 3.02, H 1.81, N 1.76, Na 1.45, W 60.75; found: C 2.95, H 1.31, N 1.72, Na 1.39, W 60.8.

Crystal data and structure refinements for **1**: $H_{102}K_8Na_2O_{117}Pd_3Te_2W_{18}$, MW = 6217.08 gmol^{-1}; red block crystal: $0.07\times0.06\times0.02$ mm^3. Tetragonal, space group $P\bar{4}2_1m$, $a = 16.9647(7)$, $c = 13.8221(10)$ Å, $V = 3978.0(4)$ Å^3, $Z = 2$, $\rho = 4.591$ gcm^{-3}, $\lambda(Mo_{K\alpha}) = 0.71073$ mm^1, 16060 reflections measured, 3766 unique ($R_{int} = 0.1375$) which were used in all calculations. Final $R1 = 0.0450$ and $wR2 = 0.0792$ (all data). Crystal data and structure refinements for **2**: $C_{38}H_{266}N_{19}Na_{13}O_{281}Te_8W_{64}$, MW = 18571.91 gmol^{-1}; colorless needle-shaped crystal: $0.21\times0.04\times0.03$ mm^3. Monoclinic, space group $C2/c$, $a = 82.6223(18)$, $b = 15.0229(2)$, $c = 54.3205(16)$ Å, $\beta = 95.051(2)$, $V = 67162(3)$ Å^3, $Z = 8$, $\rho = 3.597$ gcm^{-3}, $\lambda(Cu_{K\alpha}) = 1.54184$ mm^1, 69833 reflections measured, 37874 unique ($R_{int} = 0.0573$) which were used in all calculations. Final $R1 = 0.0647$ and $wR2 = 0.1780$ (all data). Crystal data and structure refinements for **2′**: $C_{38}H_{306}N_{19}Cs_2Na_{11}O_{301}Te_8W_{64}$, MW = 19152.04 gmol^{-1}; colorless block crystal: $0.31\times0.08\times0.05$ mm^3. Monoclinic, space group $C2$, $a = 35.1788(6)$, $b = 38.8304(4)$, $c = 30.7129(6)$ Å, $\beta = 123.352(3)$, $V = 35044.5(10)$ Å^3, $Z = 4$, $\rho = 3.572$ gcm^{-3}, $\lambda(Mo_{K\alpha}) = 0.71073$ mm^1, 226131 reflections measured, 60631 unique ($R_{int} = 0.0759$) which were used in all calculations. Final $R1 = 0.0515$ and $wR2 = 0.1345$ (all data). Crystal data and structure refinements for **3**: $C_{16}H_{114}N_8Na_4O_{100}Te_3W_{21}$, MW = 6354.47 gmol^{-1}; colorless block crystal: $0.35\times0.27\times0.17$ mm^3. Monoclinic, space group $P2_1/c$, $a = 14.2566(3)$, $b = 19.9994(5)$, $c = 37.9253(10)$ Å, $\beta = 93.873(2)$, $V = 10788.7(5)$ Å^3, $Z = 4$, $\rho = 3.950$ gcm^{-3}, $\lambda(Mo_{K\alpha}) = 0.71073$ mm^1, 88032 reflections measured, 21180 unique ($R_{int} = 0.0850$) which were used in all calculations. Final $R1 = 0.0634$ and $wR2 = 0.1499$ (all data). Data collection and reduction were performed using the CrysAlisPro software package and structure solution, and refinement were carried out using SHELXS-97[14] and SHELXL-97[15] using WinGX.[16] Corrections for incident and diffracted beam absorption effects were applied using analytical numeric absorption correction using a multifaceted crystal model.[17] CSD-423852 (**1**), CCDC 854719 (**2**), 854720 (**2′**) and 854721 (**3**) contains the supplementary crystallographic data for this paper. These data can be obtained free of charge from the Fachinformationszentrum Karlsruhe, 76344 Eggenstein-Leopoldshafen, Germany (fax: (+49)7247-808-666; e-mail: crysdata@fiz-karlsruhe.de) for **1** and from the Cambridge Crystallographic Data Centre via www.ccdc.cam.ac.uk/data_request/cif for **2**, **2′**, and **3**.

[1] M. T. Pope, A. Müller, *Angew. Chem.* **1991**, *103*, 56–70; *Angew. Chem. Int. Ed. Engl.* **1991**, *30*, 34–48.

[2] a) D. L. Long, R. Tsunashima, L. Cronin, *Angew. Chem.* **2010**, *122*, 1780–1803; *Angew. Chem. Int. Ed.* **2010**, *49*, 1736–1758; b) D. L. Long, E. Burkholder, L. Cronin, *Chem. Soc. Rev.* **2007**, *36*, 105–121.

[3] a) *Chem. Rev.* **1998**, *98* (special issue on polyoxometalates); b) *Polyoxometalate Chemistry: From Topology via Self-Assembly to Applications* (Eds.: M. T. Pope, A. Müller), Kluwer, Dordrecht, **2001**, pp. 1–467.

[4] a) T. M. Anderson, W. A. Neiwert, M. L. Kirk, P. M. B. Piccoli, A. J. Schultz, T. F. Koetzle, D. G. Musaev, K. Morokuma, R. Cao, C. L. Hill, *Science* **2004**, *306*, 2074–2077; b) Q. S. Yin, J. M. Tan, C. Besson, Y. V. Geletii, D. G. Musaev, A. E. Kuznetsov, Z. Luo, K. I. Hardcastle, C. L. Hill, *Science* **2010**, *328*, 342–345; c) C. P. Pradeep, D. L. Long, G. N. Newton, Y. F. Song, L. Cronin, *Angew. Chem.* **2008**, *120*, 4460–4463; *Angew. Chem. Int. Ed.* **2008**, *47*, 4388–4391; d) C. Talbot-Eeckelaers, S. J. A. Pope, A. J. Hynes, R. Copping, C. J. Jones, R. J. Taylor, S. Faulkner, D. Sykes, F. R. Livens, I. May, *J. Am. Chem. Soc.* **2007**, *129*, 2442–2443.

[5] a) D. L. Long, P. Kögerler, L. Cronin, *Angew. Chem.* **2004**, *116*, 1853–1856; *Angew. Chem. Int. Ed.* **2004**, *43*, 1817–1820; b) D. L. Long, H. Abbas, P. Kögerler, L. Cronin, *Angew. Chem.* **2005**, *117*, 3481–3485; *Angew. Chem. Int. Ed.* **2005**, *44*, 3415–3419.

[6] a) J. Yan, D. L. Long, L. Cronin, *Angew. Chem.* **2010**, *122*, 4211–4214; *Angew. Chem. Int. Ed.* **2010**, *49*, 4117–4120; b) J. Yan, J. Gao, D. L. Long, H. N. Miras, L. Cronin, *J. Am. Chem. Soc.* **2010**, *132*, 11410–11411.

[7] J. Yan, D. L. Long, E. F. Wilson, L. Cronin, *Angew. Chem.* **2009**, *121*, 4440–4444; *Angew. Chem. Int. Ed.* **2009**, *48*, 4376–4380.

[8] J. Gao, J. Yan, S. G. Mitchell, H. N. Miras, A. G. Boulay, D. L. Long, L. Cronin, *Chem. Sci.* **2011**, *2*, 1502–1508.

[9] a) L. H. Bi, U. Kortz, B. Keita, L. Nadjo, H. Borrmann, *Inorg. Chem.* **2004**, *43*, 8367–8372; b) T. M. Anderson, R. Cao, E. Slonkina, B. Hedman, K. O. Hodgson, K. I. Hardcastle, W. A. Neiwert, S. X. Wu, M. L. Kirk, S. Knottenbelt, E. C. Depperman, B. Keita, L. Nadjo, D. G. Musaev, K. Morokuma, C. L. Hill, *J. Am. Chem. Soc.* **2005**, *127*, 11948–11949.

[10] a) E. M. Limanski, D. Drewes, E. Droste, R. Böhner, B. Krebs, *J. Mol. Struct.* **2003**, *656*, 17–25; b) U. Kortz, N. K. Al-Kassem, M. G. Savelieff, N. A. A. Kadi, M. Sadakane, *Inorg. Chem.* **2001**, *40*, 4742–4749; c) U. Kortz, M. G. Savelieff, B. S. Bassil, B. Keita, L. Nadjo, *Inorg. Chem.* **2002**, *41*, 783–789; d) A. J. Gaunt, I. May, R. Copping, A. I. Bhatt, D. Collison, O. D. Fox, K. T. Holman, M. T. Pope, *Dalton Trans.* **2003**, 3009–3014.

[11] a) A. H. Ismail, N. H. Nsouli, M. H. Dickman, J. Knez, U. Kortz, *J. Cluster Sci.* **2009**, *20*, 453–465; b) C. Ritchie, K. G. Alley, C. Boskovic, *Dalton Trans.* **2010**, *39*, 8872–8874.

[12] "Syntheses and Crystal Structure Studies of Novel Selenium- and Tellurium-Substituted Lacunary Polyoxometalates": B. Krebs, E. Droste, M. Piepenbrink in *Polyoxometalate Chemistry* (Eds.: M. T. Pope, A. Müller), Kluwer, Dordrecht, **2001**.

[13] L. P. Rigdon, J. E. Harrar, *Anal. Chem.* **1974**, *46*, 696–700.

[14] G. Sheldrick, *Acta Crystallogr. Sect. A* **1990**, *46*, 467–473.

[15] G. Sheldrick, *Acta Crystallogr. Sect. A* **2008**, *64*, 112–122.

[16] L. Farrugia, *J. Appl. Crystallogr.* **1999**, *32*, 837–838.

[17] R. C. Clark, J. S. Reid, *Acta Crystallogr. Sect. A* **1995**, *51*, 887–897.